DEVELOPMENT OF ACCURATE AND PRECISE IN-VACUUM UNDULATOR SYSTEM

A. Deyhim, J. Kulesza, ADC USA, Lansing, NY 14882, U.S.A
Dr. K. Blomqvist, Brunskog, Sweden

Abstract

Typical in-vacuum undulators, especially long ones, have several associated engineering challenges to be accurate and precise; magnetic centerline stability, inner girder hangers, and magnet period to name a few. The following describes these issues in more detail and ADC's methods solved these critical issues for long in vacuum undulators. ADC has designed, built and delivered Insertion Devices and Magnetic Measurement Systems to such facilities as; MAXLab (EPU, Planar-2, and Measurement System), ALBA and Australian Synchrotron Project (Wiggler), BNL (Cryo In-Vacuum), SSRF (In-Vacuum – 2, and Measurement System), PAL (In-Vacuum and Measurement System), NSRRC (In-Vacuum), and SRC (Planar and EPU). The information presented here uses data from a recent IVU we delivered to PAL. This IVU, shown in Figure 1, will be installed at Pohang Accelerator Laboratory (PAL) for U-SAXS (Ultra Small Angle X-ray Scattering) beamline in 2011. The IVU generates undulator radiation up to ~14 keV using higher harmonic (up to 9th) undulator radiation with 2.5 GeV PLS electron beam.

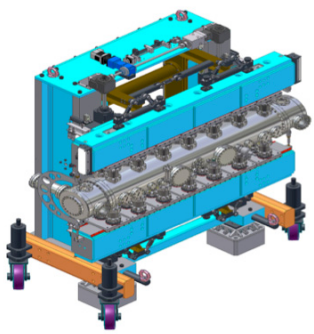

Figure 1: PAL in-vacuum undulator.

INNER GIRDER HANGERS

The inner girders are connected to the outer girders through a series of hangers. The inner magnet arrays must be shimmed without the chamber in place which means they must be removed from the outer girders to install the vacuum chamber. The inner girders are usually separated at the hangers and removed, the vacuum chamber is mounted, then the magnet arrays are slid inside the vacuum chamber and the hangers reconnected without disturbing the magnetic field. There is currently no way to measure or correct a magnet array once it has been inserted into the vacuum chamber so no changes in field can be detected until it is installed in the ring. This places great emphasis on the repeatability of the hanger reconnection. The hangers are also often used to flatten the inner girders. The standard hanger is threaded into the inner girders and the thread engagement is used to both flatten the girder and repeat the reconnection after installation in the vacuum chamber.

ADC developed a unique hanger design that employs a coupling to separate the inner and outer portions of the hanger assembly. The inner part is firmly threaded into the girder and then coupled to the outer part which is fixed to the outer girder through a set of bearing rails that allow for thermal expansion. Shim plates between the outer hanger and the bearing rail plate are ground to flatten the inner girder. The coupling is uniquely designed to connect the inner and outer shafts with sub-micron repeatability but yet have the strength to resist the varying magnet load without deflection.

On the PAL IVU, while the machine was aligned to the hall bench, ADC performed a chamber simulation test to determine the effect of dismounting the magnet array and remounting in the chamber. The magnet arrays were first set to 6 mm gap and the array holder framework was mounted. The hangers were then completely disconnected at the coupling simulating the removal of the arrays. The hangers were then reconnected and the array holder framework was removed. The gap was exercised and a small (induced) taper was corrected. The magnetic field was measured again and essentially nothing changed. The results are shown below in Table 1 which compares pre-test and post-test data for 6 mm gap.

MAGNET PERIOD

Magnet period must be controlled to produce good phase error. The installation of the magnets onto the inner girders is critical. Many internal girders have a "T" slot cut into the girder which is used to attach the magnets holders, this allows the magnets to be moved slightly to correct for period errors. The holder location must be measured and corrected as the magnets are

Table 1: Pre-Test and Post-Test Data for Chamber Simulation Test

Gap [mm]	Bpeak [T]	Beff [T]	$\delta\varphi$ [Degree]	I1x [Gcm]	I1y [Gcm]	I2x [Gcm2]	I2y [Gcm2]	NQ [G]	SQ [G]	NS [G/cm]	SS [G/cm]	NO [G/cm2]	SO [G/cm2]
Pre Test	0.90075	0.87438	2.5465	-4.736	8.980	-526	2235	-15.62	-38.22	40.324	-36.97	-38.078	51.395
Post Test	0.90164	0.87513	2.6537	-2.585	8.658	-1047	2675	-1.799	-45.72	9.475	-26.16	-78.906	58.261

mounted to provide a good starting point for the period. This is tedious work and unknown errors are propagated into subsequent magnet mounting.

ADC has developed a magnet mounting procedure that combines a dowel hole/pin in the magnet holders and a mating hole in the girder. The location of the dowel holes in both the girder and holders was excellent. The resulting period was such that the initial average was within 1-2 microns of specification. This saved us a lot of time mounting the magnets and allowed us to achieve a phase error of 2.5 degrees. While it is true that phase error derives mostly from angle error in the magnet blocks, having a good starting point for period is critical.

BEAMLINE SHIFT

The standard design for IVU frames transmits the magnet load to the frame using springs to compensate for the load at small gaps. The problem with this approach is that these loads deflect the upper and lower girders differently which can lead to a beam line shift at different gaps. The difference is due to the relative strength of the upper and lower parts of the "C" frame. The lower is generally stiffer being closer to the floor supports and the upper weaker because of the attachment near the top of the strong-back frame. Girder deflection becomes unequal and the magnetic center line shifts at different gaps.

ADC's solution is to implement a bucking frame that accepts the magnet load and transmits no load to the strong-back frame. The bucking frame is connected to the upper and lower girders through a "whiffle tree" design that distributes the connection points along the outer girder. The whiffle tree incorporates disk spring stacks that engage at larger gaps. The bucking frame is attached, at both ends, to a large brass bushing located at the magnetic centerline on the strong-back frame. This allows the bucking frame to pivot a small amount. The bucking frame actually becomes a spring at small gaps. The result is that the magnet load is resisted equally on the top and bottom girders resulting in minimal or no beam line shift.

PAL IVU

The IVU ADC built for PAL is currently in qualification. As previously mentioned, ADC applied several innovations that helped to make this machine a success. Some results are shown in Table 2 below. A design summary shows the key design points. All specifications were met.

Table 2: Design Summary

Undulator Type	Hybrid
Undulator Symmetry	Asymmetric
Undulator Period Length	20.0 mm
Number of Full Size Poles	176
Total Number of Poles	178
Length of Magnet Assemblies	1780.9 mm
Length Including Correction Magnets	≈1800 mm
Gap Range	4 – 36 mm
Beam Height	1400 mm
Effective Peak Field at 5 mm Gap	1.053 T
Effective k at 5 mm Gap	1.97
Magnetic Force at 4 mm Gap	22.8 kN
Pole Material	soft steel
Magnet Block Material	NdFeB
Magnet Supplier Shin-Etsu	N39UH
Maximum RMS Photon Phase Error	$< 5^{o}$
Max. Residual 1st Field Integral	$10x10^{-6}$ Tm
Max. Residual 2nd Field Integral	$10x10^{-6}Tm^{2}$
Max. Corrector Strength	2000 Gcm
Intrinsic Coercivity of Magnet Material	> 25 kOe
Gap Encoder Minimum Resolution	.00025 mm
Maximum Bake-Out Temperature	150 C
Deflection of Backing Beam	< 3 um
Vertical Positioning Accuracy	2 um
Average Vacuum Pressure (w/o beam)	$<1x10^{-11}$ Torr
Average Vacuum Pressure (w/ beam)	$<5x10^{-9}$ Torr
Max Pump Down Time	1 Day
Gap Velocity Range	<.005-1 mm/s
Taper Control	<.005 mm
Beam Height	1400 mm

The results of shimming can be seen for several gaps in Table 3 below. The magnets were first sorted in software by field strength. Then the first integral was measured on each block with a flip coil and the magnets were sorted again in a sequence that produced the lowest overall integral. The magnets were mounted in two different types of holders. One holder held a single magnet while another held two pole pieces and a magnet. The number and placement of the inner to outer girder hangers was optimized with an FEA. A single gap motor was used with a separate motor for taper. Two absolute linear encoders were mounted on either end of the machine on the upper girder but referenced to the lower.

The machine was shimmed with copper shims under the magnet holders and also under the poles as needed. ADC used one of our "portable" measurement systems. All analysis was done in Wavemetrics IGOR using a combination of ADC developed routine and B2E from ESRF. Several plots of data are shown in Figures 2-7 for a gap of 5 mm. No correction coils are used at this gap.

ADC is convinced that these innovations can be extended to 4 meter IVUs.

Table 3: Peak Field, Effective Field, Phase Error, 1st and 2nd Integrals, Normal and Skew Quadrupoles, Sextupoles, and Octupoles for Various Gaps

Gap [mm]	Bpeak [T]	Beff [T]	$\delta\varphi$ [Degree]	I1x [Gcm]	I1y [Gcm]	I2x [Gcm2]	I2y [Gcm2]	NQ [G]	SQ [G]	NS [G/cm]	SS [G/cm]	NO [G/cm2]	SO [G/cm2]
5	1.07945	1.03461	2.61278	-11.52	11.197	1336	-1100	-29.03	-31.501	56.28	-33.46	-65.434	65.15
6	0.90209	0.87572	2.58686	-2.948	8.369	3381	352	-27.08	-39.81	21.53	-27.96	-21.86	51.846
7	0.75801	0.74245	2.42221	4.4975	7.7361	4360	1281	-21.45	-44.02	-4.885	-35.08	17.449	44.784
8	0.60413	0.63082	2.18651	9.1956	8.2265	5100	2097	-6.8283	-47.29	-23.79	-40.39	23.948	19.594
9	0.54170	0.53609	2.01163	12.197	7.1057	5456	1978	0.0584	-50.72	-33.63	-40.13	58.818	15.246
10	0.45965	0.45621	1.80472	13.785	8.1819	6089	2650	-1.480	-58.37	-49.47	-47.65	100.045	27.721
11	0.39042	0.38834	1.88856	14.016	7.9393	5711	2860	4.5322	-57.96	-47.71	-53.04	94.702	15.205

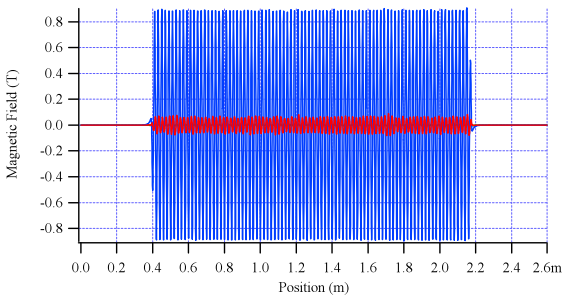

Figure 2: Raw Hall probe data.

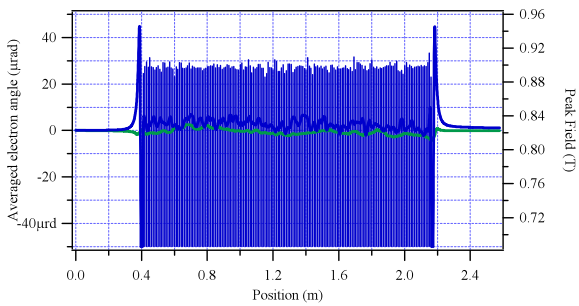

Figure 3: Averaged electron angle and peak field.

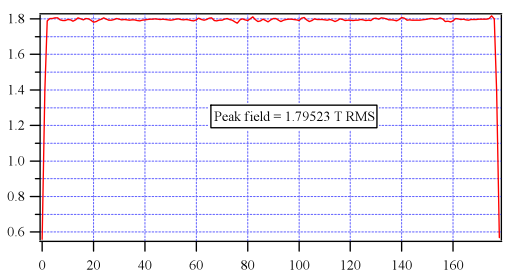

Figure 4: Peak field.

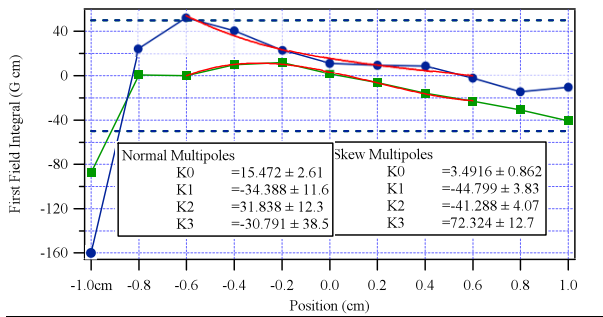

Figure 5: First integrals, normal and skew multipoles with background removed.

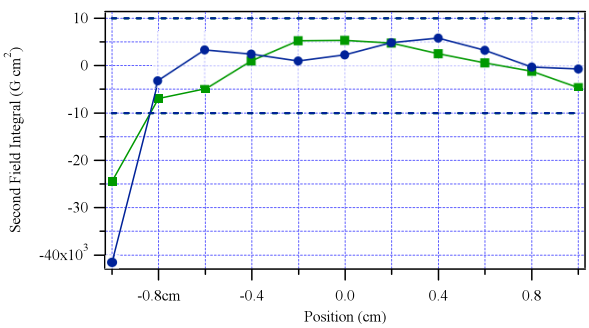

Figure 6: Second normal and skew integrals.

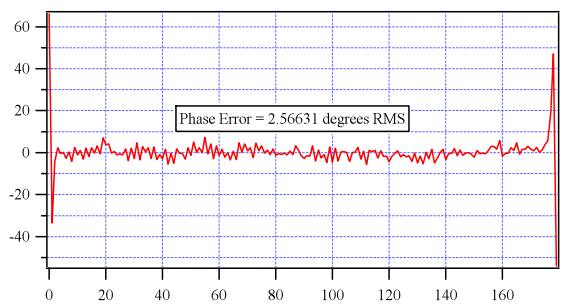

Figure 7: Phase error angle.